RESEARCH ARTICLE

Induction of Telomere Dysfunction Mediated by the Telomerase Substrate Precursor 6-Thio-2′-Deoxyguanosine

Ilgen Mender[1,2], Sergei Gryaznov[3], Z. Gunnur Dikmen[2], Woodring E. Wright[1], and Jerry W. Shay[1,4]

ABSTRACT

The relationships between telomerase and telomeres represent attractive targets for new anticancer agents. Here, we report that the nucleoside analogue 6-thio-2′-deoxyguanosine (6-thio-dG) is recognized by telomerase and is incorporated into *de novo*–synthesized telomeres. This results in modified telomeres, leading to telomere dysfunction, but only in cells expressing telomerase. 6-Thio-dG, but not 6-thioguanine, induced telomere dysfunction in telomerase-positive human cancer cells and hTERT-expressing human fibroblasts, but not in telomerase-negative cells. Treatment with 6-thio-dG resulted in rapid cell death for the vast majority of the cancer cell lines tested, whereas normal human fibroblasts and human colonic epithelial cells were largely unaffected. In A549 lung cancer cell–based mouse xenograft studies, 6-thio-dG caused a decrease in the tumor growth rate superior to that observed with 6-thioguanine treatment. In addition, 6-thio-dG increased telomere dysfunction in tumor cells *in vivo*. These results indicate that 6-thio-dG may provide a new telomere-addressed telomerase-dependent anticancer approach.

SIGNIFICANCE: Telomerase is an almost universal oncology target, yet there are few telomerase-directed therapies in human clinical trials. In the present study, we demonstrate a small-molecule telomerase substrate approach that induces telomerase-mediated targeted "telomere uncapping," but only in telomerase-positive cancer cells, with minimal effects in normal telomerase-negative cells. *Cancer Discov; 5(1); 82–95. ©2014 AACR.*

See related commentary by Wellinger, p. 19.

[1]Department of Cell Biology, The University of Texas Southwestern Medical Center, Dallas, Texas. [2]Faculty of Medicine, Department of Biochemistry, Hacettepe University, Ankara, Turkey. [3]AuraSense Therapeutics, Skokie, Illinois. [4]Center for Excellence in Genomics Medicine Research, King Abdulaziz University, Jeddah, Saudi Arabia.

Note: Supplementary data for this article are available at Cancer Discovery Online (http://cancerdiscovery.aacrjournals.org/).

Corresponding Author: Jerry W. Shay, Department of Cell Biology, UT Southwestern Medical Center, 5323 Harry Hines Boulevard, MC 9039, Dallas, TX 75930-9039. Phone: 214-648-4201; Fax: 214-648-5814; E-mail: jerry.shay@utsouthwestern.edu

doi: 10.1158/2159-8290.CD-14-0609

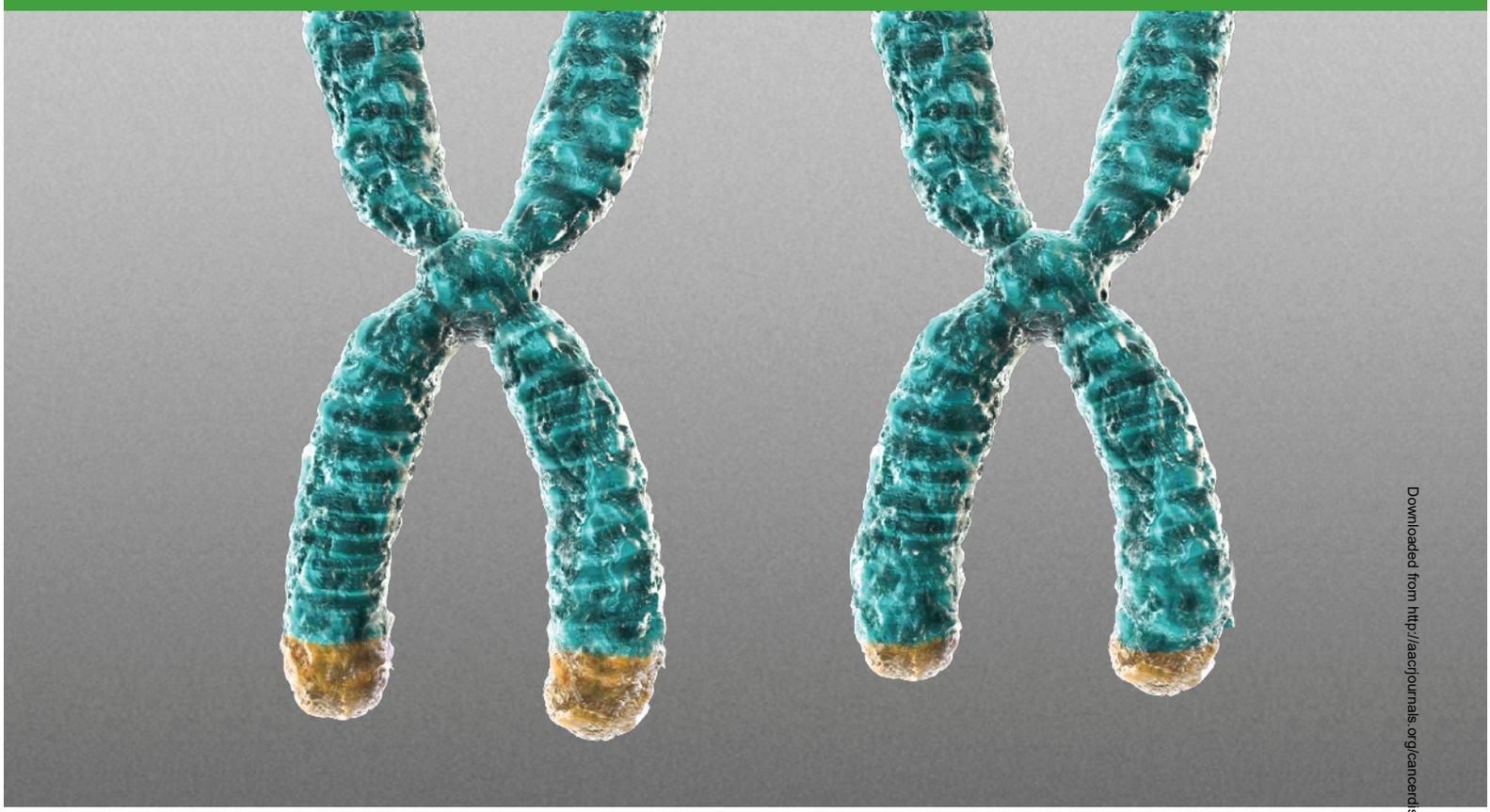

INTRODUCTION

Telomeres, which are found at the end of eukaryotic linear chromosomes, are essential for chromosome maintenance and genomic stability (1). Mammalian telomeres are composed of repetitive d-(TTAGGG) sequences and telomere-specific "shelterin" complex proteins, which protect the chromosome ends from being recognized as DNA damage and preventing end-to-end chromosomal fusions (2). The shelterin proteins (TRF1, TRF2, POT1, TIN2, TPP1, and RAP1) form a protective complex that is present at telomeres throughout the cell cycle (3). Because of the "end-replication problem," oxidative damage and other replication-associated end-processing events, telomeres progressively shorten with each round of DNA replication in normal somatic cells (4). The ribonucleoprotein enzyme complex telomerase counteracts telomere shortening by adding hexameric telomeric DNA (TTAGGG) repeats to the end of linear chromosomes in cancer cells but only partially counteracts progressive telomere shortening in some normal human proliferative stem-like cells. Telomerase has two main functional components: a protein component, hTERT (human telomerase reverse transcriptase), and a functional RNA component, hTR or hTERC (contains the telomerase template sequences, which facilitate the correct synthesis of TTAGGG repeats). Whereas most normal somatic human cells do not have telomerase activity, it is almost universally detected in approximately 85% to 90% of primary human cancers (5, 6). It is widely accepted that progressive telomere shortening in normal cells leads to replicative senescence that provides an initial barrier against tumor progression (7, 8). Many previous studies have focused on targeting telomerase activity in cancer cells (9, 10), with the rationale being that telomerase-addressed therapies might have low general toxicity, high tumor specificity, and reduced side effects as compared to other therapeutic approaches (11).

One of the leading telomerase inhibitors, GRN163L (imetelstat sodium), is a 13-mer thio-phosphoramidate oligonucleotide with the sequence 5′-TAGGGTTAGACAA-3′. The compound is complementary to the template region of the telomerase RNA subunit, hTR, and it is a highly potent, direct, and competitive telomerase inhibitor (12). Because imetelstat treatment causes progressive telomere shortening due to telomerase inhibition (9, 13–15), it has been stated that it generally requires relatively prolonged treatment period to induce therapeutically relevant tumor reduction effects (15). During this treatment period, most tumor cells will continue to grow until already-short telomeres become even shorter, and the cells eventually undergo apoptosis or growth arrest. Therefore, imetelstat treatment without any adjuvant therapy may be limited in its utility as a broad-spectrum antitumor therapy due to the prolonged lag period required to have effects. In addition, the development of imetelstat has been put on hold for solid tumors due to hematologic and hepatotoxic dose-limited side effects (16, 17). Thus, additional telomerase-dependent therapeutic approaches are not only timely but also critically needed to target cancer cell telomeres via novel mechanisms.

Dysfunctional telomeres are associated with DNA-damage response factors such as 53BP1, γ-H2AX, RAD17, ATM, and MRE11 (18). When the shelterin protein TRF2 is compromised, telomeres become dysfunctional and display DNA-damage signals that can be detected using immunofluorescence imaging techniques. These telomere-associated DNA-damage signals are referred to as telomere dysfunction–induced foci (TIF). TIFs can be visualized by colocalization of telomeres with DNA-damage response factors. Critically short telomeres, or impaired telomere-protective proteins in the shelterin complex, can lead to "uncapped" telomere structures, which in turn can induce rapid senescence, apoptosis, and/or chromosome end fusions (18–20).

Thiopurines, such as 6-thioguanine and 6-mercaptopurine, are currently used as anti-inflammatory, antileukemic, and immunosuppressive agents in clinical practice (21). Thiopurine metabolism is complex and involves both activation and inactivation reactions (22). In activation reactions, 6-thioguanine is converted to 6-thioguanosine monophosphate by the hypoxanthine guanine phosphoribosyltransferase (HPRT) enzyme. Then, 6-thioguanosine monophosphate is further metabolized to 6-thio-2′-deoxyguanosine 5′-triphosphate by kinases and RNA reductases, which may eventually be incorporated into DNA strands during DNA replication. DNA-incorporated 6-thioguanine may also generate reactive oxygen species (21, 23), which may cause additional damage to DNA, proteins, and other cellular macromolecules, and thus block cellular replication (21). Although the thiopurines are in clinical use for the treatment of some types of leukemia, their utility for solid tumor treatment has been limited, in part, due to increased toxicities and the development of other therapies.

We reasoned that it may be possible to utilize telomerase by itself as a key functional intermediary for anticancer effects, and by doing this, to decrease general nonspecific thiopurine toxicity by using 6-thioguanine–containing prodrugs (23). Because telomerase has a high affinity for guanine bases containing 2′-deoxyguanosine 5′-triphosphate, and also for DNA substrates with –GGG motifs at the 3′ terminus (such as the repetitive TTAGGG repeats in telomeres), we designed an analogue of 6-thioguanine that would be preferentially recognized by telomerase, become incorporated into *de novo* synthesized telomeres by telomerase, and lead to a relatively rapid uncapping of telomeres, resulting in TIF formation and cancer cell growth arrest or death. This may be described as a telomerase-mediated telomere-poisoning approach. Others have suggested that telomerase may recognize 6-thio-2′-deoxyguanosine 5′-triphosphate, and this molecule may be incorporated into oligonucleotide primer extension products in cell-free biochemical assays (24), but this observation has never been experimentally tested *in vitro* or *in vivo* in cancer cells or other telomerase-positive cells. We hypothesized that a key nucleoside precursor of 6-thio-2′-deoxyguanosine 5′-triphosphate, 6-thio-2′-deoxyguanosine, may be less toxic and rapidly converted to the 6-thio-2′-deoxyguanosine 5′-triphosphate in cells. Thus, in cells expressing telomerase, 6-thio-2′-deoxyguanosine 5′-triphosphate should be incorporated into *de novo*–extended telomeric products, leading to TIF formation. This would make the telomeres structurally and functionally different from native telomeres, because some guanine bases within -GGG-telomeric repeats will be replaced by 6-thio groups. These guanine base–modified telomeres, with 6-thio groups replacing 6-oxygen counterparts, while being synthesized by telomerase, would result in alteration of the overall chemistry, structure, and function of the shelterin complex (such as G-quadruplex forming properties and protein recognition; ref. 25), leading to their recognition as telomeric DNA-damage signals, but almost exclusively in cells expressing telomerase.

In this study, we evaluated 6-thio-2′-deoxyguanosine (6-thio-dG) to determine its therapeutic effects and also general toxicity in cancer and normal cells *in vitro* and *in vivo*. The activity and telomere-targeting properties of 6-thio-dG were compared with 6-thioguanine. Our results provide an experimental rationale for a potentially new cancer treatment approach based on the administration of 6-thio-dG. The approach represents a different paradigm for the treatment of telomerase-positive human cancers, irrespective of their telomere length, based on a dual mechanism of action: acute cytotoxicity derived from 6-thio-dG antimetabolic properties and its incorporation into genomic DNA, accompanied by telomeric DNA incorporation, modification, and telomere uncapping reducing the lag time for efficacy. The chemical structures of 6-thioguanine and 6-thio-dG are shown in Fig. 1A.

RESULTS

Growth Inhibition Kinetics of Colon Cancer, Non–Small Cell Lung Cancer, Alternative Lengthening of Telomeres Cells, and Normal Human Fibroblasts and Colonic Epithelial Cells

HCT116 colon and A549 lung cancer cells, along with an additional panel of non–small cell lung cancer (NSCLC) cell lines (H2882, HCC2429, HCC827, HCC15, H2087, HCC4017, HCC515, and H2009), normal human BJ fibroblasts, colonic epithelial cells (HCEC1), and alternative lengthening of telomeres cancer cells (telomerase-negative cell lines) were treated with 0.5 to 10 μmol/L 6-thio-dG and 6-thioguanine every 3 days over a 1-week period. Treatment with 6-thio-dG and 6-thioguanine resulted in the death of the vast majority of HCT116, A549, H2882, HCC2429, HCC827, HCC15, H2087, HCC4017, HCC515, and H2009 cells (in the submicromolar to low-micromolar range), whereas normal BJ fibroblasts, HCEC1 cells, and alternative lengthening of telomeres cells were less affected (higher micromolar range). The growth-inhibition results of representative images of HCT116, A549, HCC15, BJ fibroblast, HCEC1, and VA13 (alternative lengthening of telomeres) cells and the morphology of HCT116, A549, HCC15, BJ fibroblast, and HCEC1 cells following 1-week treatment are shown in Fig. 1B and C, respectively.

Effects of 6-Thio-dG and 6-Thioguanine on Cell Viability

To investigate the effect of 6-thio-dG and 6-thioguanine, we seeded HCT116 cells and 9 NSCLC-derived cell lines, as well as normal BJ fibroblast cells and HCEC1 cells, in 96-well plates, and then treated the cells with different concentrations of 6-thio-dG or 6-thioguanine every 3 days. Following 1 week of treatment (using 10 different doses of the compounds with serial dilutions), the cell viability was determined by the CellTiterGlo luminescent cell viability assay. We found that both 6-thio-dG and 6-thioguanine inhibited cell viability in a

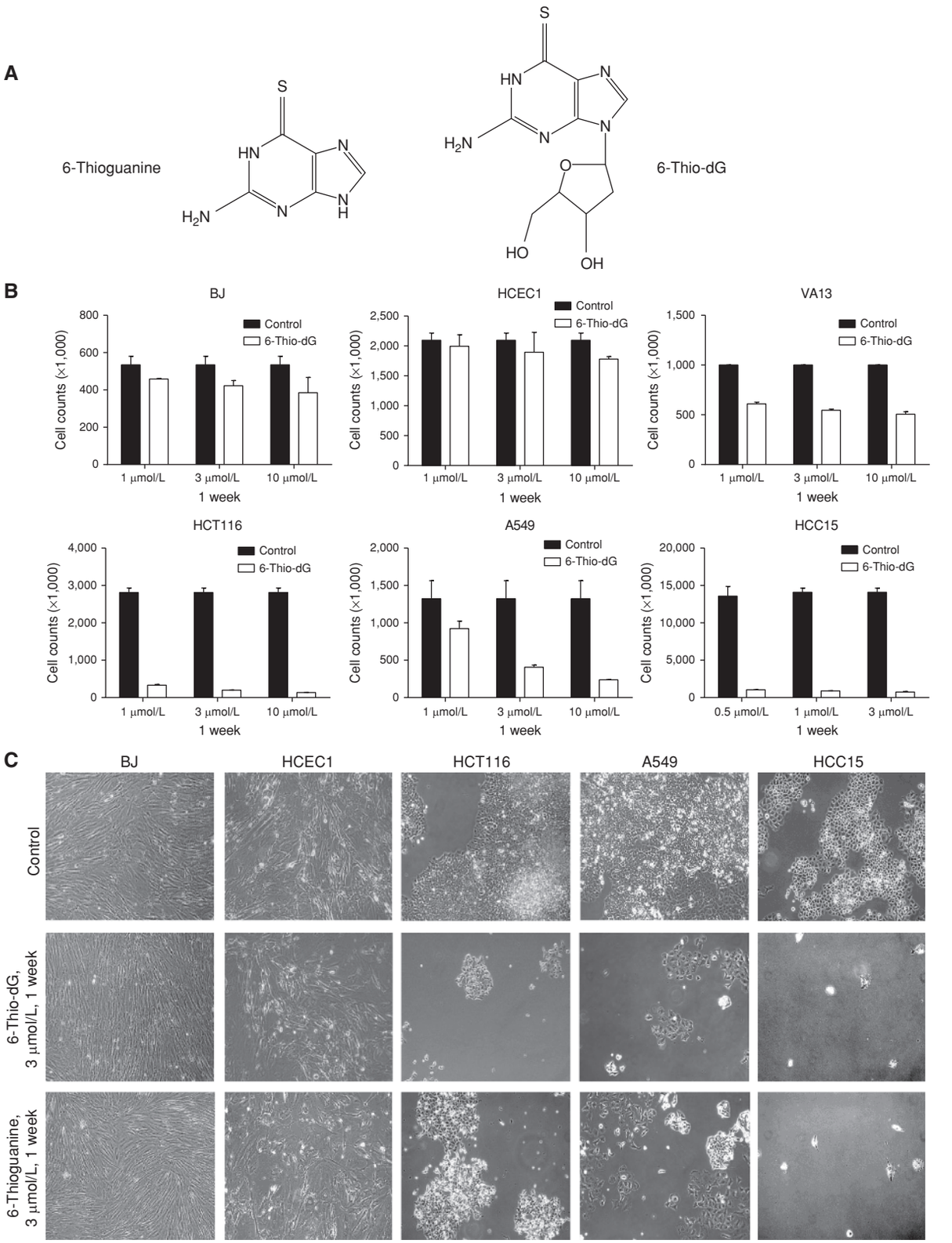

Figure 1. **A,** chemical structures of 6-thioguanine and 6-thio-dG. **B,** cell counts of BJ (normal human fibroblasts), HCEC1 (human diploid colonic epithelial cells), VA13 (telomerase-negative, alternative lengthening of telomeres cells), and HCT116, A549, and HCC15 telomerase-positive cells treated with 6-thio-dG (0.5–10 μmol/L) for 1 week (control; DMSO treated; SDs from two independent experiments). **C,** the morphology of BJ, HCEC1, HCT116, A549, and HCC15 cells treated with 6-thio-dG (3 μmol/L) and 6-thioguanine (3 μmol/L) for 1 week (treatment every 3 days).

dose-dependent manner. The IC_{50} values of all cells are summarized in Supplementary Table S1 and Supplementary Fig. S1. We observed that the cancer cells were highly sensitive to 6-thio-dG (observed IC_{50} values are between 0.7 and 2.9 μmol/L, depending on the specific cell type) and 6-thioguanine (IC_{50} values are between 0.7 and 3.5 μmol/L), whereas BJ cells and HCEC1 cells were mostly resistant to both drugs in terms of cell viability (Supplementary Fig. S1). In addition, these cell lines had a variety of telomere lengths, but cell killing was independent of initial telomere lengths (Supplementary Table S1).

6-Thio-dG Treatment Results in Telomere Dysfunction

To observe whether 6-thio-dG and 6-thioguanine treatment leads to telomere de-protection, HCT116 cells were seeded in chamber slides. Following cell attachment, 6-thio-dG (3 μmol/L) and 6-thioguanine (3 μmol/L) were either not added (0 time point) to fresh medium or added at various time points of 30 minutes, 3 hours, 12 hours, 24 hours, 48 hours, and 72 hours, and the cells were then fixed. To test whether 6-thio-dG and 6-thioguanine cause telomere dysfunction, interphase TIF analysis was conducted. Using the combination of γ-H2AX and TRF2 colocalization by immunostaining, we were able to identify and distinguish between nontelomeric genomic DNA damage and telomere-specific damage signals. 6-Thio-dG treatment induces a 7.8-fold increase in telomeric DNA damage as compared with 6-thioguanine after 72 hours (Fig. 2A and B). Because telomeric DNA represents only about 1/6,000th of the total genomic DNA, any TIFs above background would be considered highly significant. In addition to the increase in telomere damage by 6-thio-dG, there was also an overall modest increase in genomic DNA damage as compared to 6-thioguanine (Fig. 2C). In contrast, telomerase-negative normal BJ cells had less genomic and no detectable telomeric damage signals under similar treatment conditions (Fig. 2D and E). To test the initial hypothesis that DNA damage induced by 6-thio-dG at telomeres is actually telomerase dependent, we established an hTERT-expressing/telomerase activity–positive BJ cell line. Telomeric DNA-damage signals in these hTERT-positive BJ (BJ-hTERT$^+$) cells were compared to those in normal BJ cells (BJ-hTERT$^-$), both treated with 6-thio-dG (10 μmol/L) or 6-thioguanine (10 μmol/L). Following 48 hours of treatment, TIF analysis confirmed that in interphase cells, γ-H2AX and TRF2 colocalize in 3.3% (TIF ≥ 5), 4.2% (TIF ≥ 6), or 5.7% (TIF ≥ 7) of cells following 6-thio-dG treatment in BJ hTERT$^+$ cells, compared with background in telomerase activity–negative BJ cells and 6-thioguanine BJ hTERT$^+$ cells (Fig. 2D–F).

Treatment with 6-Thio-dG, but Not 6-Thioguanine, Results in Progressive Telomere Shortening in Cancer Cells

To determine whether administration of 6-thio-dG leads to progressive telomere shortening, in addition to the observed acute TIF induction, telomere lengths of the treated cells were evaluated by the terminal restriction fragment (TRF) assay. Colon cancer–derived HCT116 cells and normal BJ fibroblasts were treated with either 1 μmol/L or 10 μmol/L 6-thio-dG for 1 to 12 weeks. In addition, HCT116 cells were also treated with either 1 μmol/L or 10 μmol/L 6-thioguanine for 1 to 10 weeks to determine whether it has effects on telomere length maintenance. We found that telomere shortening was detectable as early as in 1 week in surviving cells, with more dramatic telomeric shortening after 12 weeks of continuous treatment with 6-thio-dG (Fig. 3A). However, administration of 6-thioguanine did not result in any significant effect on the telomere length of HCT116 cells (Fig. 3B). This suggests that intracellular metabolic pathways of 6-thio-dG and 6-thioguanine are different, and that 6-thio-dG may be much more readily converted into the corresponding 5′-triphosphate, which is being recognized by telomerase and incorporated into telomeres. In addition, BJ-hTERT$^-$ fibroblast cells treated for 10 weeks with 6-thio-dG (Fig. 3C), or 6-thioguanine (data not shown), did not show enhanced telomere shortening, as compared to untreated control cells. When telomerase activity of HCT116 cells treated with 6-thio-dG was evaluated [by the *in vitro* telomeric repeat amplification protocol (TRAP) assay], no inhibition of telomerase activity was observed for 6-thio-dG (Fig. 3D) or 6-thioguanine (data not shown). This indicates that 6-thio-dG does not directly inhibit the telomerase holoenzyme, but causes progressive telomere shortening in cells that are not immediately killed by 6-thio-dG via a mechanism independent from telomerase inhibition in HCT116 cells.

Determination of 6-Thio-dG's General Toxicity *In Vivo*

To determine an appropriate drug concentration for *in vivo* efficacy studies, we initiated experiments with 129S2 wild-type female mice using different drug concentrations to determine the general toxicity of 6-thio-dG. It was reported that 6-thioguanine doses above 3 mg/kg are toxic for mice (26). Based on this report, we chose the highest dose as 5 mg/kg (Fig. 4A) and the lowest dose as 1.67 mg/kg (Fig. 4B), for daily i.p. injections into mice, for 25 days. Following 17 days of treatment, three mice treated with 5 mg/kg of 6-thioguanine died. The mice treated with 1.67 mg/kg of 6-thioguanine did not gain weight and started to lose weight by day 24 of treatment. In contrast, 5 mg/kg of 6-thio-dG treatment did not cause any mouse deaths, and the average animal weight was stable over the 25-day course of treatment. Moreover, we did not observe any animal deaths or weight loss in the lower-dose group (1.67 mg/kg) of 6-thio-dG–treated mice (Fig. 4A and B). Based on these *in vivo* dose-defining results, we initiated mice xenograft efficacy experiments with 2 mg/kg 6-thio-dG dose.

Evaluation of 6-Thio-dG Effect on Hematologic Counts, Liver and Kidney Function Tests, and Organ Histologic Analysis

To determine whether there are toxicity differences between 6-thio-dG and 6-thioguanine beyond weight loss, wild-type female (129S2) mice were injected i.p. every 2 days at a dose of 2 mg/kg of 6-thio-dG and 6-thioguanine for a total of 14 days. Two days after the last injection, mice were sacrificed, and whole blood was collected via cardiac draw. Red blood cell (RBC) counts, white blood cell (WBC) counts, hemoglobin (Hgb), lymphocytes, hematocrit (HCT), monocytes, neutrophils, and basophils were evaluated. In addition, alanine aminotransferase (ALT)/aspartate aminotransferase (AST) for liver function, and creatinine (CREA)/urea nitrogen (BUN) for kidney function were evaluated in serum.

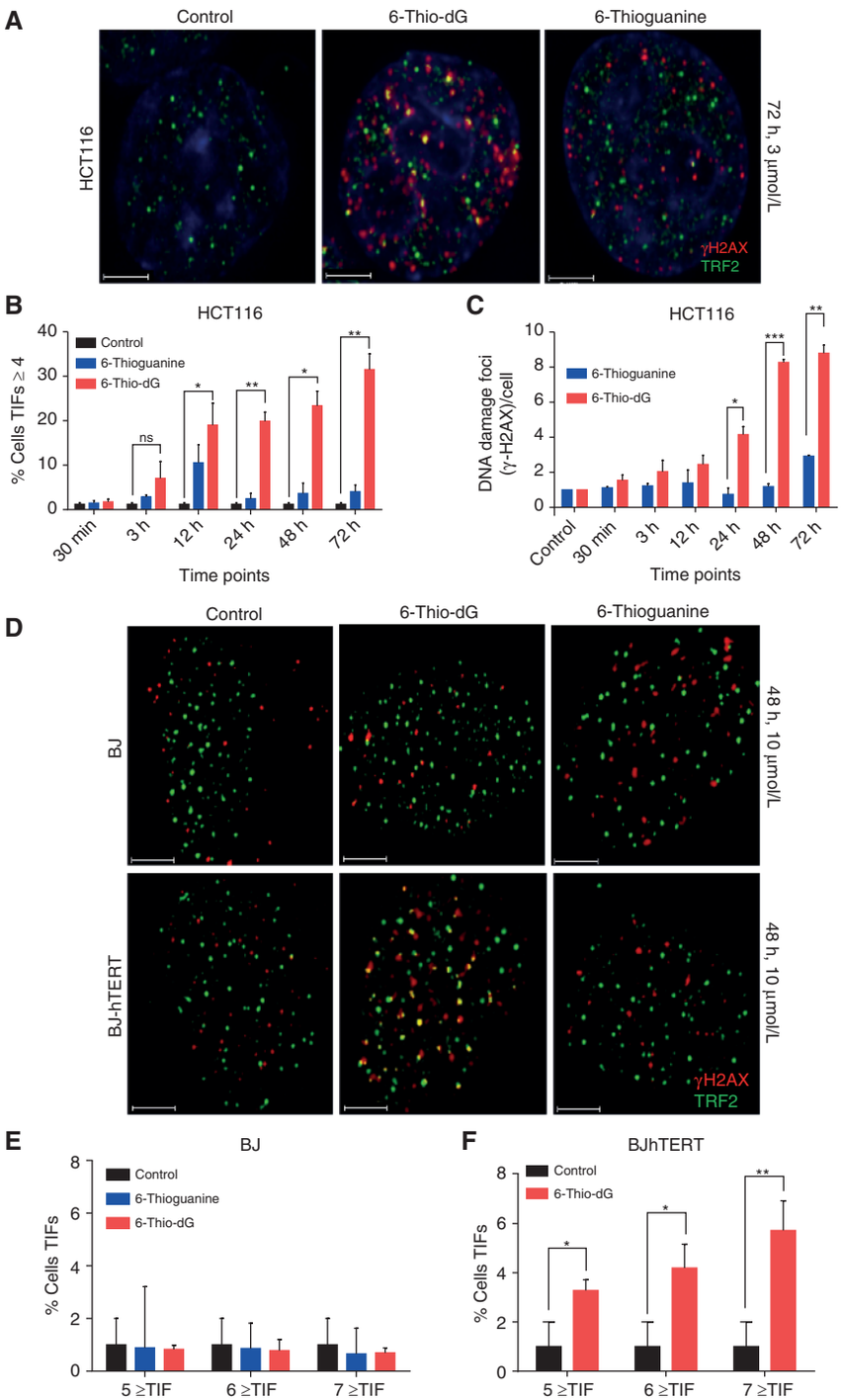

Figure 2. DNA-damage (γ-H2AX) and telomere damage–induced foci (TIFs). **A,** 6-thio-dG induced telomeric localization of γ-H2AX in HCT116 cells (with 3 μmol/L treatment), but not 6-thioguanine (with 3 μmol/L treatment). **B,** TIF index (percentage of TIF-positive cells) of HCT116 cells treated with 6-thio-dG (3 μmol/L) or 6-thioguanine (3 μmol/L). Cells with four or more γ-H2AX foci colocalizing with TRF2 were scored as TIF positive by Imaris software ($n > 55$ for HCT116; SDs from two independent experiments). *, $P < 0.05$; **, $P = 0.006$ (compared with vehicle control); ns, not significant differences in the unpaired Student *t* test. (control; untreated). **C,** DNA-damage foci per cell. HCT116 cells treated with 6-thio-dG (3 μmol/L) and 6-thioguanine (3 μmol/L) ($n > 55$; SDs from two independent experiments). **, $P = 0.003$; ***, $P = 0.0005$; *, $P = 0.0141$ (6-thio-dG:6-thioguanine); ns, not significant differences in the unpaired Student *t* test (control; DMSO treated). **D–F,** representative images (**D**) and quantitative TIF analysis following 6-thio-dG (10 μmol/L) and 6-thioguanine (10 μmol/L) treatment in BJ-hTERT⁻ (**E**) and for 6-thio-dG in BJ-hTERT⁺ cells (**F**) are shown. 6-Thio-dG induced telomeric localization of γ-H2AX in BJ-hTERT⁺ cells, but not in BJ-hTERT⁻ cells. 6-Thioguanine did not significantly induce telomeric localization of γ-H2AX in BJ-hTERT⁺ and BJ-hTERT⁻ cells ($n = 85$ for control; $n = 83$ for 6-thio-dG BJ-hTERT⁻; and $n = 81$ for 6-thioguanine–treated BJ-hTERT⁻ experiments; SDs are from two independent experiments for BJ-hTERT⁻ and three independent experiments for BJ-hTERT⁺ cells). Images were obtained by DeltaVision and then deconvoluted by Autoquant X3. DNA was stained with DAPI (blue). Red dots show DNA damage (γ-H2AX), green dots show TRF2, and yellow dots show TIF (DNA damage colocalizing with telomeres) in merged images. *, $P < 0.02$; **, $P = 0.064$ (control: 6-thio-dG) in the unpaired Student *t* test. Scale bars, 5 μm.

6-Thio-dG and 6-thioguanine did not cause any hematologic toxic effects on ALT, BUN, or CREA levels except minor neutropenia (Supplementary Fig. S2). Interestingly, although 6-thio-dG did not alter AST levels, 6-thioguanine (the already-approved compound) caused a slight increase of AST enzyme levels, which is one of the markers to show toxic effect on liver function, yet this increase was not statistically significant. In addition, we evaluated the histopathology of the liver, kidney, spleen, and colon and did not observe any toxic effect with 6-thio-dG treatment compared to control (Supplementary Fig. S3). We did observe some necrosis in the liver after 6-thioguanine treatment (data not shown).

6-Thio-dG Treatment Decreases the Tumorigenicity of A549 Cells *In Vivo*

To assess anticancer activity of 6-thio-dG and 6-thioguanine *in vivo*, we used an A549 lung cancer cell line–derived xenograft murine model. During the *in vivo* treatment phase of the

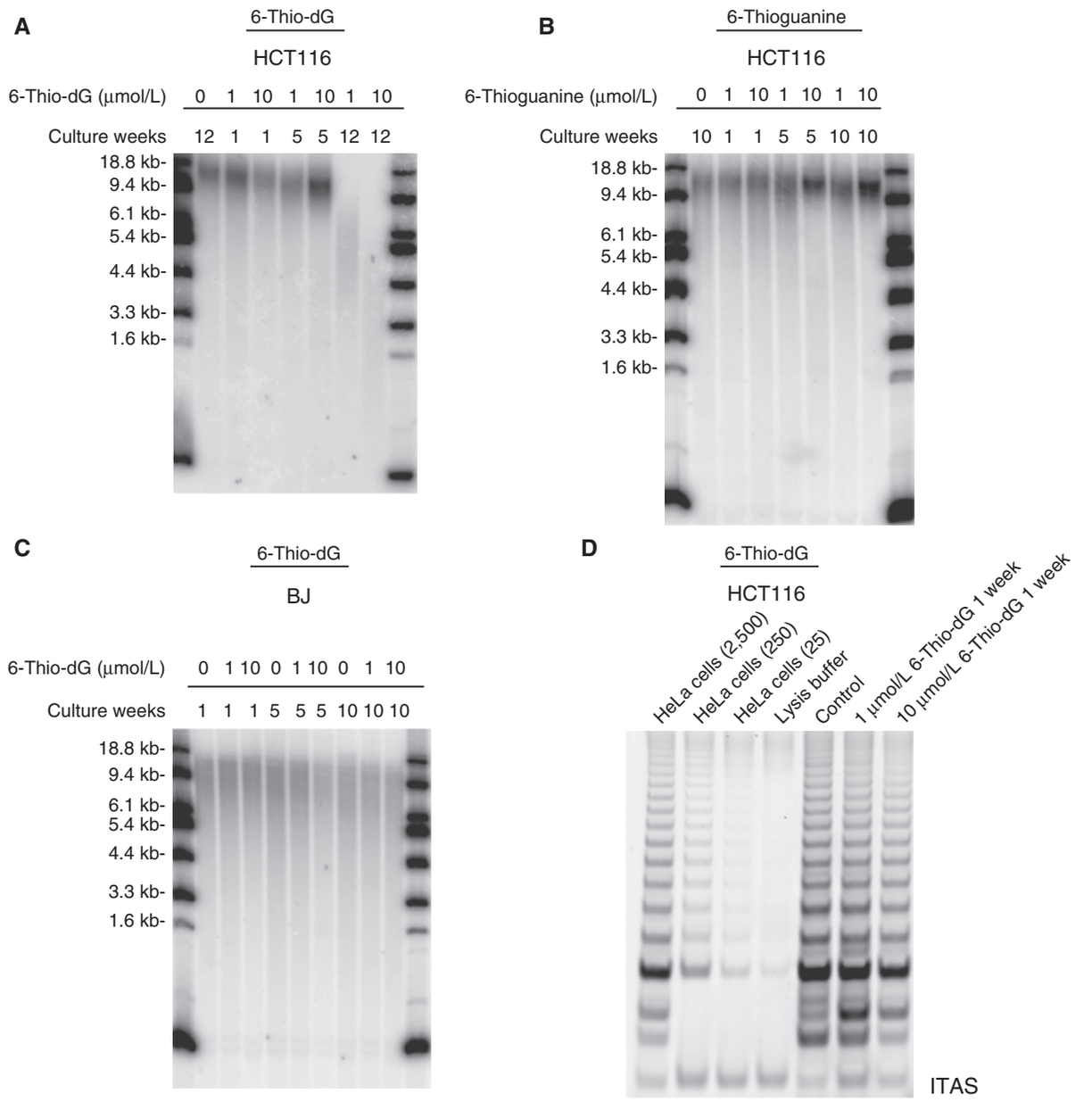

Figure 3. TRF and TRAP analysis. **A–C,** HCT116 and BJ cells treated with 6-thio-dG or 6-thioguanine. Cells were treated with 1 to 10 μmol/L of 6-thio-dG or 6-thioguanine every 3 days for the indicated number of weeks. Each week samples were collected for TRF analysis at 1×10^6 cells per sample. **D,** TRAP analysis of HCT116 cells treated with 6-thio-dG. Cells were treated with 1 and 10 μmol/L 6-thio-dG every 3 days for 1 week. The samples were collected for TRAP analysis at 1×10^5 cells per sample. TRF lengths are expressed as kilobase pairs (control; untreated). ITAS, internal telomerase assay standard.

experiments, 2 mg/kg of 6-thio-dG or 6-thioguanine [approximately 7 (μmol/L)/kg or 12 (μmol/L)/kg, respectively] was injected i.p. every other day. Tumors were first established in mice and then treatments were initiated. We observed a complete prevention of progressive tumor growth by administration of 6-thio-dG, as compared to controls or 6-thioguanine–treated animal groups (Fig. 5A). We also evaluated Ki67 staining in these tumor samples treated with 6-thio-dG and 6-thioguanine compared to controls. Ki67 is a biomarker that correlates with proliferation levels. We observed that 6-thio-dG treatment caused a decrease in Ki67 staining, compared to 6-thioguanine and controls, which may in part explain the difference of tumor growth rate using similar doses of 6-thio-dG and 6-thioguanine (Supplementary Fig. S4). To test whether local injection into the tumor was more effective in comparison with i.p. injection, we injected intratumorally (i.t.) 2.5 mg/kg of 6-thio-dG or 6-thioguanine daily for 17 days. The 6-thio-dG tumor growth rate showed even more dramatic decreases compared to 6-thioguanine or untreated controls (Fig. 5B). Importantly, residual small tumors from the 6-thio-dG–treated mice were generally highly vascularized with infiltrating inflammatory cells (Fig. 5C).

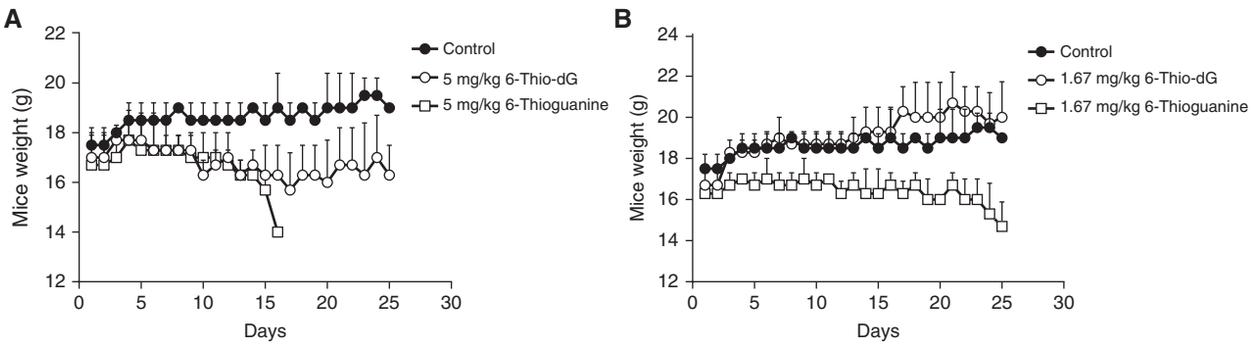

Figure 4. Wild-type mice weight following 6-thio-dG and 6-thioguanine treatment. **A,** 5 mg/kg of 6-thio-dG (compared with DMSO/PBS or 5 mg/kg of 6-thioguanine). **B,** 1.67 mg/kg of 6-thio-dG (compared with DMSO/PBS or 1.67 mg/kg of 6-thioguanine) was injected i.p. into the 129S female wild-type mice for 25 days. The mice weight (g) was scaled every day ($n = 3$).

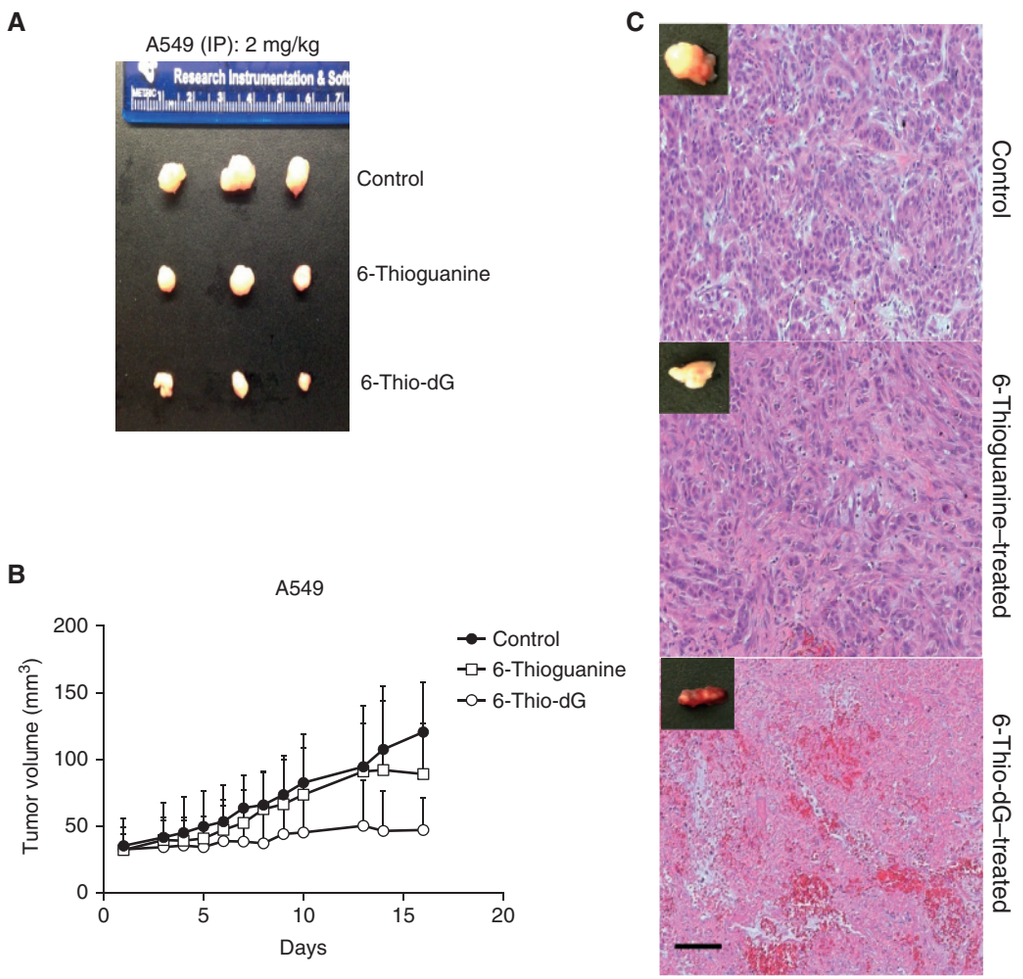

Figure 5. Intraperitoneal or intratumoral injection of 6-thio-dG or 6-thioguanine. **A,** 2 mg/kg of 6-thio-dG or 6-thioguanine injected to the A549-derived tumor for 17 days every 2 days, intraperitoneally. Representative images of isolated tumors are shown. **B,** the tumor volume (mm^3) after 2.5 mg/kg of 6-thio-dG or 6-thioguanine injection i.t. every day for 17 days. Tumor size was measured with calipers and recorded either every day or every 2 days. Tumor volumes were calculated by taking length to be the longest diameter across the tumor and width to be the corresponding perpendicular diameter, using the following formula: (length × width^2) $mm^2 \times 0.5$. **C,** the images with hematoxylin and eosin at the end of i.t. injection (control: DMSO/PBS). Note the increased inflammatory and red blood cells infiltrating the 6-thio-dG residual tumor mass at sacrifice (17 days). Magnifications, ×10; scale bar, 100 μm.

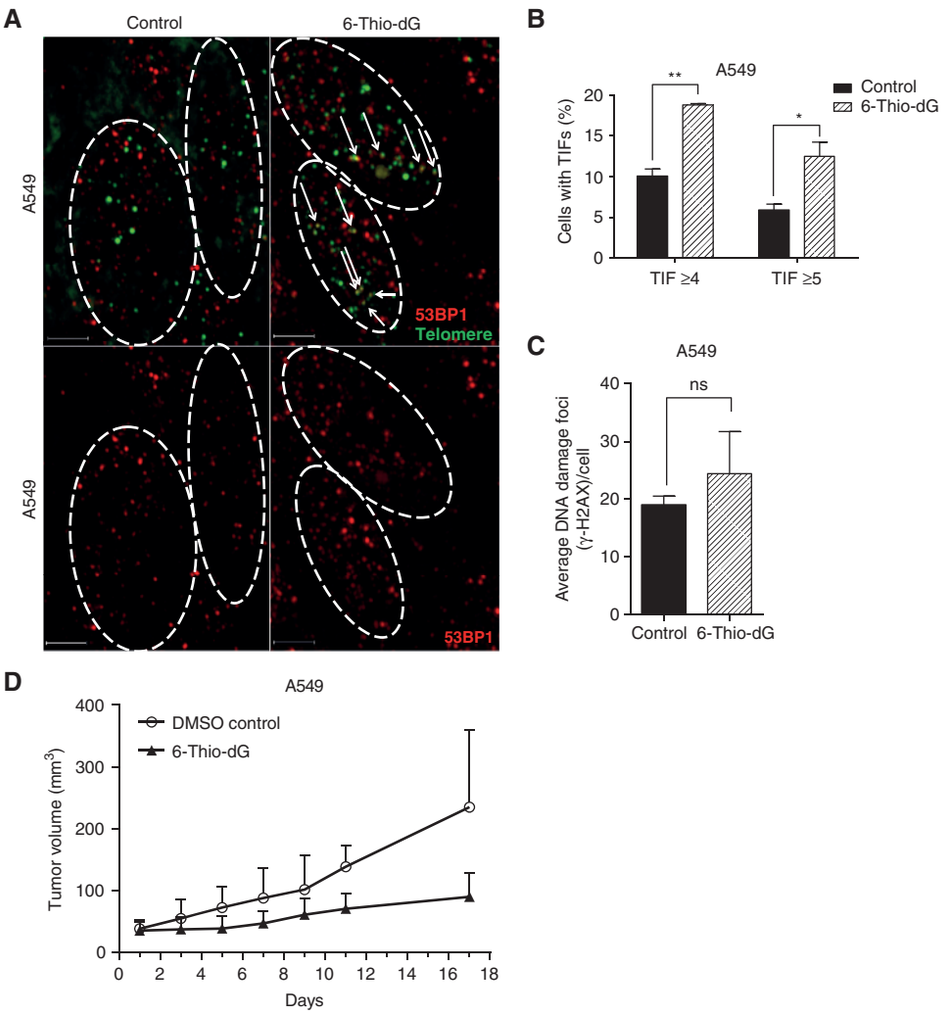

Figure 6. Binding of 53BP1 on uncapped telomeres. **A,** 6-thio-dG induced telomeric localization of 53BP1 in A549-derived tumor cells (representative data). Images were obtained by DeltaVision and then deconvoluted by Autoquant X3. Red dots show DNA damage (53BP1), green dots show telomeres, and yellow dots show TIF (DNA damage on telomeres) in merged images. Scale bars, 3 μm. **B,** TIF index (percentage of TIF-positive cells) of A549-derived tumor cells treated with 6-thio-dG. Cells with ≥4 or ≥5 53BP1 foci colocalizing with telomere were scored as TIF positive by Imaris software ($n > 150$ for control, $n > 200$ for 6-thio-dG treatment). SDs from two independent experiments. **, $P = 0.0051$; *, $P < 0.05$ (compared with control), in the unpaired Student *t* test. **C,** DNA-damage foci per cell. A549-derived tumor cells treated with 6-thio-dG ($n > 150$ for control, $n > 200$ for 6-thio-dG treatment; SDs from two independent experiments). ns, not significant differences in the unpaired Student *t* test (control vs. 6-thio-dG; control; DMSO treated). **D,** the tumor volume (mm^3) of A549-derived tumor with 6-thio-dG administration. 2 mg/kg of 6-thio-dG or DMSO/PBS was injected to the A549-derived tumor for 17 days every 2 days, intraperitoneally.

6-Thio-dG–Mediated Tumor Growth Rate Reduction Correlates with Telomere Dysfunction *In Vivo*

To test whether 6-thio-dG causes telomere dysfunction in tumor cells, 2 mg/kg of 6-thio-dG was injected i.p. every other day for 17 days. Tumor cells were then scored for TIFs. 6-Thio-dG caused a significant ~2-fold induction in TIFs compared to control (when counting positive cells as those that have TIF ≥ 4 and TIF ≥ 5), demonstrating that 6-thio-dG alters the telomere structure and function in A549-derived tumors *in vivo* (Fig. 6A and B). In addition, there was no significant difference in ongoing general DNA damage between the 6-thio-dG–treated group and control tumor cells (Fig. 6C). Overall, we observed that reduction of tumor growth rate by 6-thio-dG (Fig. 6D) correlates with telomere dysfunction *in vivo*.

DISCUSSION

Purine analogues, such as 6-thioguanine and 6-mercaptopurine, are chemotherapeutic agents that can be converted into nucleotide analogues *in vivo*. Clinically used nucleoside base analogues are nucleoside mono-, di-, and tri-phosphate prodrug forms and also antimetabolite agents. One of the main problems with these compounds is their relatively high toxicity toward normal noncancerous cells. In addition, the therapeutic effectiveness toward the majority of solid tumors is relatively low (27). Thus, 6-thioguanine is not widely used in current cancer treatment protocols, mainly due to the low drug efficacy and dose-limiting toxic side effects (28). In addition, patients with Crohn disease or leukemia being treated with 6-thioguanine can develop hepatotoxicity such as liver veno-occlusive disease. Thus, slight increases in AST levels from the mice treated with 6-thioguanine, but not 6-thio-dG, may reflect different toxicity profiles and partially explain the increased efficacy of 6-thio-dG over 6-thioguanine in the present experiments. The enzyme hypoxanthine guanine phosphoribosyl transferase (HGPRT) produces 6-thio-2′-*ribo*-guanosine 5′-monophosphate from 6-thioguanine, both *in vitro* and *in vivo*. Following this conversion, 6-thio-2′-*deoxy*-guanosine 5′-triphosphate (6-thio-dGTP) is formed by a series of transformations, catalyzed by kinases and RNA nucleotide reductases. 6-Thio-dGTP is then incorporated into *de novo*–synthesized DNA, resulting in DNA damage, followed by cell-cycle arrest and apoptosis. Cytotoxicity of 6-thio-dGTP is specific for the S-phase of the cell cycle (29). Moreover, the substitution of 2′-deoxyguanosine by 6-thio-dG in G-rich

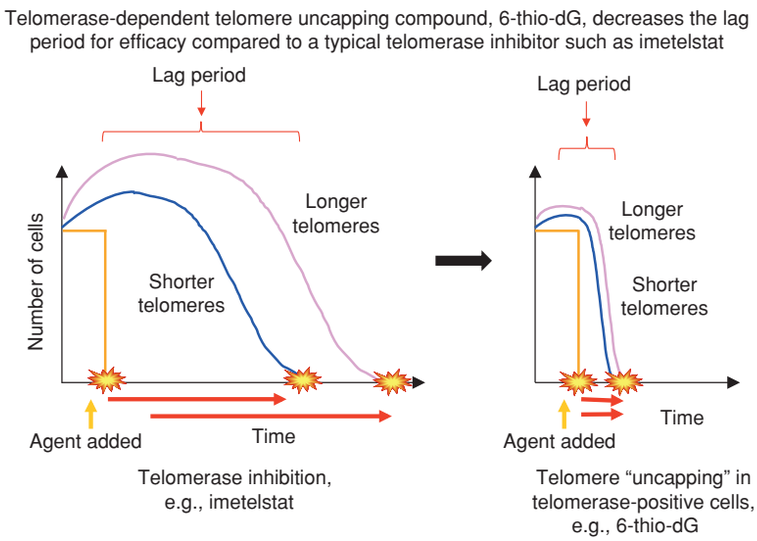

Figure 7. The efficacy of telomerase inhibition–based therapies, such as imetelstat, depends on the tumor telomere length at the beginning of treatment. The tumors with longer telomeres require a longer treatment period (longer lag period) to have therapeutic effects compared to tumors with shorter telomeres (left). Tumor telomeres (with shorter or longer) start gradually shortening with telomerase inhibition targeted agents. This leads to delay of effect (e.g., tumor shrinkage) and potentially generates adverse effects (such as increased toxicities) due to the long treatment period. However, adding a telomerase-mediated telomere uncapping agent such as 6-thio-dG results in a much quicker effect that reduces the lag period irrespective of tumor initial telomere length (right). The gold line would represent an ideal chemotherapeutic agent demonstrating an immediate reduction in tumor volume.

oligodeoxyribonucleotides inhibits the formation of G-tetrad structures in DNA (30). These studies suggest that the 5′-triphosphate form of 6-thio-dG may be able to interact with telomerase, be incorporated into the telomeres, and lead to the disruption of telomere structure and function much more effectively compared with 6-thioguanine.

Most of the single-agent anticancer therapies have not been very effective in clinical practice yet, largely due to the development of drug resistance, leading to cancer recurrences and metastasis. One of the main limitations for the potential clinical success of imetelstat, a potent telomerase inhibitor, is variable telomere lengths in the tumor cells of the treated patients. This limitation requires a relatively prolonged treatment regimen, resulting in hematologic side effects. Several human clinical trials combining imetelstat with other chemotherapeutic drugs for solid tumors have been terminated primarily due to the observed toxicities in patients (16, 17). Thus, initial tumor telomere length variability and a substantial "lag period" are the main limitations for telomerase inhibitor–based therapy (Fig. 7, left). Therefore, additional new approaches need to be evaluated that aim to increase overall therapeutic efficacy, accompanied by fewer side effects. In the current study, we have focused on the heterocyclic guanine base, modified nucleoside analogue, -6-thio-dG. In contrast with other telomerase inhibitor–based therapies, 6-thio-dG is not a direct telomerase inhibitor *per se*, but a precursor of the telomerase substrate 6-thio-dGTP. We demonstrated in the current studies that administration of this molecule, both *in vitro* and *in vivo*, significantly shortened the lag period (Fig. 7, right) by causing telomere uncapping, leading to cancer cell death independent of the initial tumor telomere length.

In the present study, we found that 6-thio-dGTP, which is formed in cells from 6-thio-dG, is efficiently recognized by telomerase and is incorporated into telomeres. This guanine base–modified nucleoside incorporation led to the marked increase in TIFs in HCT116 and BJ hTERT$^+$ cells, but not in telomerase-silent normal BJ hTERT$^-$ cells, indicating that this effect is mostly telomerase dependent. The incorporation of 6-thio-dG into telomeres and also into genomic DNA shows that the compound may have a bifunctional mode of action, targeting both telomeric and genomic DNA, in addition to acting as a potential nucleoside antimetabolite. Importantly, at therapeutically relevant doses, we did not observe any significant toxicity in normal BJ or HCEC1 cells for 6-thio-dG, demonstrating good selectivity of 6-thio-dG toward telomerase-positive cancer cells. We also observed progressive telomere shortening with 6-thio-dG in the remaining or surviving cells not immediately killed by drug treatment, which was not based on telomerase inhibition as demonstrated by *in vitro* TRAP assay. In addition to the *in vitro* studies, *in vivo* studies with wild-type mice and in mouse xenografts demonstrated less toxicity (lack of weight loss, no changes in hematologic, renal, or liver functions except minor neutropenia) and more efficacy with 6-thio-dG in comparison with DMSO control- or 6-thioguanine–treated mice. We believe that these toxicity differences on weight loss may be because of the differences in the structure of 6-thioguanine (a heterocyclic base) and 6-thio-dG (a nucleoside). Whereas 6-thioguanine participates in multiple intracellular biochemical and metabolic processes, including purine nucleoside biochemical synthesis in cells (21), 6-thio-dG may participate in fewer biochemical and metabolic processes. Also, differences in biodistribution, relative solubility (i.e., 6-thio-dG is more hydrophilic compared to 6-thioguanine), plasma protein binding, and major organ accumulation *in vivo* may also contribute to the observed toxicity differences.

Previous studies show that telomere dysfunction is a hallmark of senescence and in some instances can lead to apoptotic cell death (18, 31). Telomere dysfunction–induced senescence or apoptosis can limit tumor growth in animal models (32, 33). DNA replication stress–induced telomere dysfunction can prevent progression of cancer in precancerous lesions and limit growth rate in cancers (34). In the present study, we demonstrate that dysfunctional telomeres (TIFs) in 6-thio-dG–treated tumor cells (A549-derived) were significantly increased, compared with control tumor cells *in vivo* (A549-derived). This suggests that 6-thio-dG can be incorporated into telomeres (~1/6,000th of the genome) during replication and consequently arrest tumor growth in response to telomere dysfunction–induced checkpoints.

Interestingly, we did not observe any significant difference between control- and 6-thio-dG–treated A549-derived tumor cells *in vivo* on general DNA damage, whereas 6-thio-dG increased general DNA damage in HCT116 cells compared to control *in vitro*. This demonstrates that some cancer cells have ongoing DNA-damage signaling *in vivo* that is being repaired but that 6-thio-dG–induced telomere DNA damage may not be easily repaired.

Although effects on telomerase-positive stem cells are a potential concern for advancing 6-thio-dG to human clinical trials, pilot *in vivo* toxicity testing at effective doses did not reveal any significant hematologic, renal, or gastrointestinal system rate-limiting side effects. Whereas there are likely to be some effects of 6-thio-dG on transient amplifying telomerase-positive cells, quiescent stem cells are known to be telomerase silent and unlikely to be affected by 6-thio-dG. Other potential side effects will be further addressed in broader in-depth toxicology testing as this molecule is advanced through formal preclinical investigational new drug–enabling studies. Thus, because 6-thio-dG will be most likely used in clinical trials over a much shorter time period compared to imetelstat, any side effects observed may be transient. In conclusion, this study provides the first experimental evidence for the bifunctional mechanism of action for the nucleoside analogue 6-thio-dG, targeting both genomic and telomeric DNA and rapid cancer cell death irrespective of the initial cancer telomere length *in vitro*. Moreover, administration of 6-thio-dG has a profound effect in reducing the tumor growth rate following telomere dysfunction in mouse xenograft cancer models.

These findings provide an initial scientific rationale for the development of new clinical cancer treatment approaches based on targeting telomeres in telomerase-positive cancer cells. In the minimal residual disease setting, where cancer relapse is often a predicted outcome, modified nucleoside molecules, such as 6-thio-dG, may prevent or delay the recurrence of the disease. In addition, in the maintenance setting, along with other chemotherapeutic agents, 6-thio-dG may be more efficacious, while offering lower overall toxicity.

METHODS

Cell Lines

The panel of authenticated NSCLC cell lines (H2882, HCC2429, HCC827, HCC15, H2087, HCC4017, HCC515, and H2009) was provided by John D. Minna (The University of Texas Southwestern Medical Center, Dallas, TX). HCT116 human colon cells, A549 human NSCLC cells, the panel of additional NSCLC cell lines (H2882, HCC2429, HCC827, HCC15, H2087, HCC4017, HCC515, and H2009), and BJ human fibroblasts were grown in medium X (DMEM:199, 4:1; HyClone) supplemented with 10% Cosmic Calf Serum (HyClone) without antibiotic. HCEC1 cells were cultured in medium consisting of medium X supplemented with 2% Cosmic Calf Serum and insulin. BJ and HCEC1 cells were cultured at 37°C in low oxygen (2%–5%). BJ cells were immortalized by transfection of a retroviral hTERT-TK-hygromycin cassette. Successful hTERT-hygromycin expression was confirmed in clones by testing for hygromycin resistance and the presence of telomerase activity. All NSCLC lines listed above and used in these studies were obtained from the Hamon Cancer Center Collection (The University of Texas Southwestern Medical Center, Dallas, TX) and have been DNA fingerprinted using the PowerPlex 1.2 Kit (Promega) and found *Mycoplasma* free using the e-Myco Kit (Boca Scientific). All cells were compared to the complete database in our own collection and that of the ATCC. The HCT116 cell line was directly obtained from the ATCC but not reauthenticated by the authors. The BJ and HCEC1 cells were each shown to contain a normal diploid karyotype and found to be *Mycoplasma* free but beyond that not authenticated by the authors.

Drug Preparation

6-Thio-dG (Metkinen Oy) and 6-thioguanine (Sigma) were dissolved in DMSO/water (1:2) to prepare 50 mmol/L or 10 mmol/L stock solutions, which were kept frozen at −20°C. Once *in vitro* experiments were conducted, a 1 mmol/L final concentration was prepared in serum-free medium and added at varying amounts for cell treatments. For mouse *in vivo* studies, drugs were prepared in a 5% DMSO solution.

Cell Viability Assay

HCT116 cells (0.5×10^3 cells/well), A549 cells (0.6×10^3 cells/well), H2882, HCC2429, HCC827, HCC15, H2087, HCC4017, HCC515, and H2009 cells (1.5×10^3 cells/well), and BJ and HCEC1 cells (2×10^3 cells/well) were plated in growth media in 96-well plates. Cells were incubated for 1 week and treated with varying concentrations of 6-thio-dG and 6-thioguanine or DMSO every 3 days. The 96-well plates were analyzed according the manufacturer's directions for the CellTiterGlo luminescent cell viability assay (Promega) to obtain IC_{50} values. The IC_{50} is defined as the concentration of drug at which 50% of the cells are inhibited by the drug. Sigmoidal dose–response curves (GraphPad Prism) were used to calculate IC_{50} values. All samples were analyzed in triplicate, and SDs are from two independent experiments.

Long-Term Cell Culture Studies

For long-term cellular experiments, HCT116 (1×10^3 cells/cm^2) and BJ (1×10^4 cells/cm^2) cells were treated with 6-thio-dG (1, 3, and 10 μmol/L) containing medium every 3 days. The cells were counted and replated approximately every week for 10 to 12 weeks. In addition, HCT116 cells (1×10^3 cells/cm^2) were fed with 6-thioguanine (1, 3, and 10 μmol/L) every 3 days, cells were counted weekly, 1×10^6 cells were collected for TRF analysis, and the remainder were replated or cryopreserved.

Telomerase Activity Assay

Telomerase activity was measured by the TRAP assay (35). Briefly, HCT116 cells were treated with 1 or 10 μmol/L of 6-thio-dG for 1 week. Cells (1×10^5) were then collected and lysed with ice-cold NP-40 lysis buffer (10 mmol/L Tris–HCl, pH 8.0, 1.0 mmol/L $MgCl_2$, 1 mmol/L EDTA, 1% NP-40, 0.25 mmol/L sodium deoxycholate, 10% glycerol, 150 mmol/L NaCl, 5 mmol/L β-mercaptoethanol) for 30 minutes. One microliter cellular lysate was used for each reaction. HeLa cells were used as a positive control, and lysis buffer was used as a negative control. Telomerase extension products were amplified using PCR (95°C for 5 minutes to inactivate telomerase, then 95°C for 30 seconds, 52°C for 30 seconds, 72°C for 30 seconds; 24 cycles). Samples were run on a 10% non-denaturating acrylamide gel and visualized using a Typhoon PhosphorImager scanner system (Molecular Dynamics; GE Healthcare) that is capable of reading Cy5 fluorescence.

Telomere Length Assay (TRF)

Cells (1×10^6) were collected and washed with PBS. DNA was isolated using the DNeasy blood and tissue kit according to the manufacturer's instructions (#69506, Qiagen). DNA (2.5 μg) was digested with six different restriction enzymes (HhaI, HinfI, MspI, HaeIII, RsaI, and AluI; New England Biolabs) and incubated at 37°C overnight. Digested DNA was separated on a 0.7% agarose gel overnight at 70 V. The TRF gel was placed in denaturating solution for 20 minutes (0.5 mol/L NaOH, 1.5 mol/L NaCl, pH 13.2) and dried on

Whatman 3-MM paper under vacuum for 3 hours at 56°C. The gel was then placed for 15 minutes in neutralization buffer (1.5 mol/L NaCl, 0.5 mol/L Tris–HCl, pH 8.0) and then probed with a radiolabeled telomeric probe (C-rich) for 16 hours at 42°C in 5× saline-sodium citrate (SSC) buffer, 5× Denhardt solution, 10 (mmol/L)/L Na_2HPO_4, and 1 (mmol/L)/L $Na_2H_2P_20_7$. The gel was washed once with 2× SSC, 0.1% SDS; twice with 0.5× SSC, 0.1% SDS; and then twice with 0.5× SSC, 1% SDS at room temperature for 15 minutes. Gels were exposed to a PhosphorImager screen overnight and analyzed using a Typhoon PhosphorImager scanner system (Molecular Dynamics). ImageQuant and GraphPad prism were used to determine average telomere length of cells.

TIF Assay

The TIF assay is based on the colocalization detection of DNA damage by an antibody against broken double-stranded DNA, such as γ-H2AX, and telomeres using an antibody against the telomeric shelterin protein TRF2. Briefly, HCT116 cells were plated in 4-well chamber slides, and after the cells attached to the surface, either 3 μmol/L of 6-thio-dG or 3 μmol/L of 6-thioguanine was added to the medium at different time points (0, 30 minutes, 3 hours, 12 hours, 24 hours, 48 hours, and 72 hours). BJ hTERT$^-$ and BJ hTERT$^+$ cells were plated in 4-well chamber slides, and after the cells attached to the surface, either 10 μmol/L of 6-thio-dG or 10 μmol/L of 6-thioguanine was added to the medium for 48 hours. Slides were rinsed once with PBS and fixed in 4% paraformaldehyde in PBS for 10 minutes. Then, cells were washed twice with PBS and permeabilized in 0.5% Nonidet-P40 in PBS, blocked with 0.5% BSA and 0.2% fish gelatin in PBS for 30 minutes. Anti-γH2AX (mouse; Millipore) was diluted 1:1,000 and anti-TRF2 (rabbit; Abcam) was diluted 1:200 in blocking solution, and this primary antibody mixture was incubated on cells for 2 hours. Following 3 washes with PBST (1× PBS in 0.1% Triton) and 3 washes with PBS, cells were incubated with Alexa Fluor 488–conjugated goat anti-rabbit (1:500; Invitrogen) and Alexa Fluor 568–conjugated goat anti-mouse (1:500; Invitrogen) for 40 minutes, then washed 6 times with PBS. After drying, the slides were mounted with Vectashield mounting medium with 4′,6-diamidino-2-phenylindole (DAPI; Vector Laboratories). Images were captured with Deltavision wide-field microscope using the 60× objective, then deconvoluted using Autoquant X3. TIFs were quantified using Imaris software.

Drug Toxicity Animal Experiments

All procedures and experiments involving mice were approved by The University of Texas Southwestern Institutional Animal Care and Use Committee and conducted as per institutional guidelines. Wild-type female 129S2 mice were used to determine a 6-thio-dG drug toxicity curve. Mice were randomly divided to control, 6-thio-dG, and 6-thioguanine treatment groups. Animals were injected i.p. every day at a dose of 5 mg/kg or 1.67 mg/kg in 100 μL DMSO/PBS mixture per mouse. Animals were weighed and observed every day for 25 days ($n = 3$).

Histology and Serum Analysis

Wild-type female 129S2 mice were used for histology and serum analysis. Mice were randomly divided into control, 6-thio-dG, and 6-thioguanine treatment groups. Animals were injected i.p. every 2 days at a dose of 2 mg/kg in 100 μL DMSO/PBS mixture per mouse for 14 days and sacrificed 2 days after the last injection. After euthanasia by CO_2, a panel of tissues and organs was fixed in 10% neutral buffered formalin. Fixed tissues were embedded in paraffin, sectioned at 5-μm thickness, and stained with hematoxylin and eosin. The following tissues were examined: liver, kidney, spleen, and colon. Images were captured with Axiovision software v4.6.3 on an Axioskop 2 Plus microscope mounted with an AxioCamHR color camera (Carl Zeiss Microscopy) using Plan-APOCHROM 20× objectives; scale bars, 100 μm. For hematologic analysis, whole blood was collected via cardiac draw in Sarstedt 100 μL K3E EDTA tubes and immediately analyzed for RBC and WBC counts, Hgb, HCT, and differential WBC lymphocytes, monocytes, neutrophils, and basophils using an automated IDEXX ProCyte DX Hematology analyzer (IDEXX Laboratories, Inc.). All biochemical serum evaluations used to investigate organ functions were performed at the same time to minimize analytical variability, and determined on a Vitros 250 Analyzer (Ortho Clinical Diagnostics, Johnson & Johnson Co.). We evaluated a liver enzyme panel (AST and ALT) and a kidney enzyme panel (CREA and BUN).

Establishment of Xenograft Models

A subcutaneous xenograft mouse model of the human A549 NSCLC was used to evaluate the effects of 6-thio-dG and 6-thioguanine treatment *in vivo*. Athymic NCR nu/nu female mice (~6-week-old) were used (National Cancer Institute, Bethesda, MD). A total of 2.5×10^6 A549 cells were inoculated subcutaneously into the left and right dorsal flanks of the nude mice in 100 μL PBS. When tumors reached approximately 40 mm^3 average volume, mice were randomly divided into control, 6-thio-dG, and 6-thioguanine treatment groups (3 animals in each group). Animals were injected i.p. every 2 days for 17 days at a dose of 2 mg/kg in 100 μL DMSO/PBS mixture per mouse. In addition, different animals were injected i.t. every day for 16 days at a dose of 2.5 mg/kg in 50 μL DMSO/PBS mixture per mouse. Tumor size was measured by calipers and recorded either every day or every 2 days. Tumor volumes were calculated by taking length to be the longest diameter across the tumor and width to be the corresponding perpendicular diameter, using the following formula: $(\text{length} \times \text{width}^2)\ mm^2 \times 0.5$. No animal died during the experimental period. The animals were sacrificed by CO_2 inhalation 24 hours after the last dose of treatment. The tumors were resected, fixed with 4% paraformaldehyde, and paraffin-embedded for sectioning and immunohistochemistry staining.

Ki67 Proliferation Assay

Tissues were processed, paraffin-embedded, and cut into 5-μm sections. Sections were deparaffinized, rehydrated, and then antigens retrieved with citrate buffer [10 (mmol/L)/L sodium citrate, pH 6.0; 0.05% Tween 20] in a GE microwave oven (model 1540WW002) at power 5 (20 minutes). Endogenous peroxidase, biotin, and proteins were sequentially blocked with solutions of 3% hydrogen peroxide (Sigma-Aldrich), the Avidin/Biotin Blocking Kit (Vector Laboratories), and 10% BSA (Vector Laboratories). Anti-Ki67 primary antibody (1:1,000) was diluted in 1× PBS, and then sections were incubated 30 minutes at room temperature. After washing with PBS, secondary antibody and ABC reagent were applied using the VECTASTAIN ABC Kit (Vector Laboratories) following the manufacturer's protocol. Tissue sections were then incubated with ImmPACT DAB peroxidase substrate (Vector Laboratories), counterstained with hematoxylin, and then dried overnight before coverslip mounting. Images were captured with Axiovision software v4.6.3 on an Axioskop 2 Plus microscope with an AxioCamHR color camera (Carl Zeiss Microscopy) using Plan-APOCHROM 20×, 40× and 63× objectives; scale bars, 100 μm.

ImmunoFISH

Tissue sections were processed for TIF analysis by FISH as described previously (34). Briefly, 5-μm tissue sections were deparaffinized by sequential washes in xylene (2 × 5 minutes), 100% ethanol (2 × 2 minutes), 95% ethanol (1 × 2 minutes), 75% ethanol (1 × 2 minutes), and 50% ethanol (1 × 2 minutes) and then washed with tap water (2 × 3 minutes). Deparaffinized tissue sections were incubated in sodium citrate buffer (10 mmol/L Na-citrate, 0.05% Tween 20, pH 6.0) in a microwave (power 5) for 20 minutes to retrieve antigens. After tissue sections cooled down, they were rinsed with 1× PBS for 5 minutes and then dehydrated in 95% ethanol for 3 minutes. After

air-drying, denaturation was conducted with hybridization buffer containing FITC-conjugated telomere sequence $(TTAGGG)_3$–specific peptide nucleic acid (PNA) probe (PNA Bio), 70% formamide, 12 mmol/L Tris–HCl, pH 8.0, 0.5 mmol/L KCl, 1 mmol/L $MgCl_2$, 0.08% Triton X-100, and 0.25% BSA for 5 minutes at 80°C, followed by 2-hour incubation in the same buffer at 37°C. Slides were washed sequentially with 70% formamide (Ambion; Life Technologies)/0.6 × SSC (Invitrogen; 3 × 15 minutes), 2 × SSC (1 × 15 minutes), PBS (1 × 5 minutes), and PBST (PBS + 0.1% Tween 20; 1 × 5 minutes) and incubated with blocking buffer (4% BSA in PBST) for 30 minutes. Sections were incubated with primary polyclonal anti-53BP1 antibody (1:500; Novus Bio) in blocking buffer at room temperature for 1 hour. Following washes with PBST (2 × 5 minutes), tissue sections were incubated with Alexa Fluor 568–conjugated goat anti-rabbit (1:500; Invitrogen) in blocking buffer at room temperature for 1 hour. Sections were washed sequentially with PBST (3 × 5 minutes) and PBS (1 × 5 minutes). The slides were mounted with Vectashield mounting medium with DAPI. Images were captured with a Deltavision wide-field microscope using a 100× objective, then deconvoluted using Autoquant X3. TIFs were quantified using Imaris software.

Immunohistochemical Analysis

Formalin-fixed, paraffin-embedded tissue was used for immunohistochemical analyses. Sections were cut to 5 μm, deparaffinized, and stained with hematoxylin I and eosin Y (Fisher Scientific).

Statistical Analysis

The observed data are presented as mean values ± SD. SDs were shown only above the line to make the graphs more clear. Comparisons of different groups for statistical significance were analyzed using a two-tailed, unpaired Student *t* test. A *P* value of 0.05 or less was considered significant. Statistical analyses were performed using GraphPad Prism software version 6.01.

Disclosure of Potential Conflicts of Interest

No potential conflicts of interest were disclosed.

Authors' Contributions

Conception and design: I. Mender, S. Gryaznov, Z.G. Dikmen, J.W. Shay
Development of methodology: I. Mender, J.W. Shay
Acquisition of data (provided animals, acquired and managed patients, provided facilities, etc.): I. Mender, J.W. Shay
Analysis and interpretation of data (e.g., statistical analysis, biostatistics, computational analysis): I. Mender, S. Gryaznov, J.W. Shay
Writing, review, and/or revision of the manuscript: I. Mender, S. Gryaznov, Z.G. Dikmen, W.E. Wright
Administrative, technical, or material support (i.e., reporting or organizing data, constructing databases): S. Gryaznov
Study supervision: W.E. Wright, J.W. Shay

Grant Support

I. Mender was supported by the Scientific and Technological Research Council of Turkey (TUBITAK). This study was supported in part by NCI SPORE P50CA70907; Simmons Cancer Center Support Grant 5P30 CA142543; and the Southland Financial Corporation Distinguished Chair in Geriatric Research (J.W. Shay and W.E. Wright). This work was performed in a space constructed with support from National Institute of Health grant C06 RR30414.

The costs of publication of this article were defrayed in part by the payment of page charges. This article must therefore be hereby marked *advertisement* in accordance with 18 U.S.C. Section 1734 solely to indicate this fact.

Received June 13, 2014; revised October 8, 2014; accepted October 9, 2014; published OnlineFirst December 16, 2014.

REFERENCES

1. Naito T, Matsuura A, Ishikawa F. Circular chromosome formation in a fission yeast mutant defective in two ATM homologues. Nat Genet 1998;20:203–6.
2. Griffith JD, Comeau L, Rosenfield S, Stansel RM, Bianchi A, Moss H, et al. Mammalian telomeres end in a large duplex loop. Cell 1999;97:503–14.
3. de Lange T. Shelterin: the protein complex that shapes and safeguards human telomeres. Genes Dev 2005;19:2100–10.
4. Watson JD. Origin of concatemeric T7 DNA. Nat New Biol 1972;239:197–201.
5. Shay JW, Wright WE. Telomerase activity in human cancer. Curr Opin Oncol 1996;8:66–71.
6. Shay JW, Wright WE. Telomeres and telomerase: implications for cancer and aging. Radiat Res 2001;155:188–93.
7. Shay JW, Wright WE, Werbin H. Defining the molecular mechanisms of human cell immortalization. Biochim Biophys Acta 1991;1072:1–7.
8. Wright WE, Shay JW. Time, telomeres and tumours: is cellular senescence more than an anticancer mechanism? Trends Cell Biol 1995;5:293–7.
9. Dikmen ZG, Gellert GC, Jackson S, Gryaznov S, Tressler R, Dogan P, et al. *In vivo* inhibition of lung cancer by GRN163L: a novel human telomerase inhibitor. Cancer Res 2005;65:7866–73.
10. Bechter OE, Zou Y, Walker W, Wright WE, Shay JW. Telomeric recombination in mismatch repair deficient human colon cancer cells after telomerase inhibition. Cancer Res 2004;64:3444–51.
11. Shay JW, Wright WE. Role of telomeres and telomerase in cancer. Semin Cancer Biol 2011;21:349–53.
12. Gryaznov SM, Jackson S, Dikmen G, Harley C, Herbert BS, Wright WE, et al. Oligonucleotide conjugate GRN163L targeting human telomerase as potential anticancer and antimetastatic agent. Nucleosides Nucleotides Nucleic Acids 2007;26:1577–9.
13. Djojosubroto MW, Chin AC, Go N, Schaetzlein S, Manns MP, Gryaznov S, et al. Telomerase antagonists GRN163 and GRN163L inhibit tumor growth and increase chemosensitivity of human hepatoma. Hepatology 2005;42:1127–36.
14. Hochreiter AE, Xiao H, Goldblatt EM, Gryaznov SM, Miller KD, Badve S, et al. Telomerase template antagonist GRN163L disrupts telomere maintenance, tumor growth, and metastasis of breast cancer. Clin Cancer Res 2006;12:3184–92.
15. Gellert GC, Dikmen ZG, Wright WE, Gryaznov S, Shay JW. Effects of a novel telomerase inhibitor, GRN163L, in human breast cancer. Breast Cancer Res Treat 2006;96:73–81.
16. Williams SC. No end in sight for telomerase-targeted cancer drugs. Nat Med 2013;19:6.
17. Thompson PA, Drissi R, Muscal JA, Panditharatna E, Fouladi M, Ingle AM, et al. A phase I trial of imetelstat in children with refractory or recurrent solid tumors: a Children's Oncology Group Phase I Consortium Study (ADVL1112). Clin Cancer Res 2013;19:6578–84.
18. Takai H, Smogorzewska A, de Lange T. DNA damage foci at dysfunctional telomeres. Curr Biol 2003;13:1549–56.
19. de Lange T. Protection of mammalian telomeres. Oncogene 2002;21:532–40.
20. Karlseder J, Broccoli D, Dai Y, Hardy S, de Lange T. p53- and ATM-dependent apoptosis induced by telomeres lacking TRF2. Science 1999;283:1321–5.
21. Karran P, Attard N. Thiopurines in current medical practice: molecular mechanisms and contributions to therapy-related cancer. Nat Rev Cancer 2008;8:24–36.
22. Wang L, Weinshilboum R. Thiopurine S-methyltransferase pharmacogenetics: insights, challenges and future directions. Oncogene 2006;25:1629–38.
23. Gunnarsdottir S, Elfarra AA. Distinct tissue distribution of metabolites of the novel glutathione-activated thiopurine prodrugs

cis-6-(2-acetylvinylthio)purine and trans-6-(2-acetylvinylthio)guanine and 6-thioguanine in the mouse. Drug Metab Dispos 2003;31:718–26.
24. Tendian SW, Parker WB. Interaction of deoxyguanosine nucleotide analogs with human telomerase. Mol Pharmacol 2000;57:695–9.
25. Stefl R, Spackova N, Berger I, Koca J, Sponer J. Molecular dynamics of DNA quadruplex molecules containing inosine, 6-thioguanine and 6-thiopurine. Biophys J 2001;80:455–68.
26. Issaeva N, Thomas HD, Djureinovic T, Jaspers JE, Stoimenov I, Kyle S, et al. 6-thioguanine selectively kills BRCA2-defective tumors and overcomes PARP inhibitor resistance. Cancer Res 2010;70:6268–76.
27. Tang B, Testa JR, Kruger WD. Increasing the therapeutic index of 5-fluorouracil and 6-thioguanine by targeting loss of MTAP in tumor cells. Cancer Biol Ther 2012;13:1082–90.
28. Brem R, Karran P. Oxidation-mediated DNA cross-linking contributes to the toxicity of 6-thioguanine in human cells. Cancer Res 2012;72:4787–95.
29. Sahasranaman S, Howard D, Roy S. Clinical pharmacology and pharmacogenetics of thiopurines. Eur J Clin Pharmacol 2008;64:753–67.
30. Rao TS, Durland RH, Seth DM, Myrick MA, Bodepudi V, Revankar GR. Incorporation of 2′-deoxy-6-thioguanosine into G-rich oligodeoxyribonucleotides inhibits G-tetrad formation and facilitates triplex formation. Biochemistry 1995;34:765–72.
31. Campisi J. Cellular senescence as a tumor-suppressor mechanism. Trends Cell Biol 2001;11:S27–31.
32. Cosme-Blanco W, Shen MF, Lazar AJ, Pathak S, Lozano G, Multani AS, et al. Telomere dysfunction suppresses spontaneous tumorigenesis *in vivo* by initiating p53-dependent cellular senescence. EMBO Rep 2007;8:497–503.
33. Feldser DM, Greider CW. Short telomeres limit tumor progression *in vivo* by inducing senescence. Cancer Cell 2007;11:461–9.
34. Suram A, Kaplunov J, Patel PL, Ruan H, Cerutti A, Boccardi V, et al. Oncogene-induced telomere dysfunction enforces cellular senescence in human cancer precursor lesions. EMBO J 2012;31:2839–51.
35. Shay JW, Bacchetti S. A survey of telomerase activity in human cancer. Eur J Cancer 1997;33:787–91.